



Effect of Post Heated TiN Coating on Pitting Corrosion of Austenitic Stainless Steel

Cheng-Hsun Hsu^{*}, Hong-Tsair Liu, Wei-Che Huang and Meng-Ru Lin

Department of Materials Engineering, Tatung University, Taipei 104, Taiwan

Abstract: This study used cathodic arc deposition technique to coat TiN film on 316L austenitic stainless steel, and then the coated specimens were heat-treated at the different temperatures. Observation of coating morphology and corrosion tests were conducted for exploring the effect of post-heating temperature on composition, microstructure, and corrosion behavior of the coatings. The results showed when the heating temperature was up to the range of 500-600 °C, a Ti-N-O mixed film consisting of the two TiO₂ and TiN phases was formed on the outer layer. Particular, the film heated at 500 °C had a dense structure as well as homogeneous chemical composition. Such the result could effectively inhibit pitting corrosion of 316L stainless steel in 3.5 wt% NaCl and 10 vol% HCl solutions.

Received on 04-11-2015
 Accepted on 08-12-2015
 Published on 05-01-2016

Keywords: Cathodic arc deposition, TiN film, 316L stainless steel, Post-heating, Pitting corrosion.

DOI: <http://dx.doi.org/10.6000/2369-3355.2015.02.03.4>

1. INTRODUCTION

It is well known that stainless steels process well corrosion resistance, oxidation resistance and formability, particular austenitic stainless steels, which have been widely used in various engineering applications and high quality goods, such as surgery instruments, artificial joints, and precision watches [1]. Despite these advantages, however, the steels still have some shortcomings, such as low hardness and pitting corrosion in chlorine environment [2-5]. Physical vapor deposition (PVD) technology has become a popular method of surface treatment for several decades, because this method allows at low processing temperatures to deposit ceramic coatings on metallic substrates [6]. For example, various nitride films such as TiN, CrN, ZrN, TiAlN, and their combination could be successfully coated on austenitic stainless steels by PVD method to enhance surface property [7-11]. In particular, titanium nitride (TiN) not only has an intrinsic golden color, but also exhibits high hardness, good thermal and electrical conductivity. Such the attractive properties, thus TiN becomes an important film material in engineering applications [12]. Furthermore, some researchers utilized oxygen addition to form Ti-N-O film by sputtering for varying TiN coating color, structure and hardness. Impressively, color altered from golden type to dark blue with an increase of oxygen addition in the Ti-N-O coatings [13, 14]. A past study [15] also used cathodic arc deposition (CAD) system varying O₂/N₂ ratio of reactive

gases to synthesize Ti-N-O coatings. The result showed when the O₂/N₂ ratio was controlled at 0.25, a dense Ti-N-O film was obtained to effectively increase the wear resistance of AISI 304 stainless steel. Another previous study [16], TiN films after annealing to form Ti-N-O phase could also improve tribological property of austenitic stainless steel. According to the experimental result, we are interested to continue explore the effect of Ti-N-O film on pitting corrosion of austenitic stainless steel.

Thereby, the purpose in the study is to coat TiN films on austenitic stainless steel by CAD method along with post heat treatment at different temperatures. Coating structure, composition, roughness, and adhesion were all analyzed. In addition, the corrosion tests were carried out to evaluate the effect of post-heating temperature on the corrosion behavior of the coated specimens.

2. EXPERIMENTAL PROCEDURES

In this study, AISI 316L stainless steel was adopted as the experimental material and machined as the substrates with a diameter of 15 mm×15 mm×5 mm in size. Prior to deposition, the substrates were polished, degreased, ultrasonically cleaned, rinsed with alcohol, and dried by warm air. The base vacuum was approximately 9×10⁻³ Pa. The bombardments of argon ion at the bias of -700 V for 10 min were carried out to further ensure good adhesion of the deposited films. Two opposite titanium targets (99.99% purity) were mounted at the both sides of the chamber, while the reactive gas of N₂ was used to deposit TiN film. Before TiN coating, a pure Ti-

^{*}Department of Materials Engineering, Tatung University, Taipei 104, Taiwan; Tel: (886-2)-2586-6410; E-mail: chhsu@ttu.edu.tw

interlayer was deposited for enhancing the adhesion between TiN and substrate. The distance between the target and substrate was 150 mm. The other deposition parameters were also selected as follows: the N₂ flow rate = 50 sccm, the substrate bias voltage = -150 V, the evaporation current = 60 A, the substrate temperature = 270 °C, the holder rotation rate = 4 rpm, and depositing time = 40 min. After coating, post heat treatments of the TiN-coated specimens were separately carried out at 400, 500, and 600 °C for 2 hours in an air furnace. According to the three temperatures, the heated TiN coatings in this paper were marked as TiN(400), TiN(500), and TiN(600), respectively.

A field emission scanning electron microscopy (FESEM, LEO 1530) was used at an accelerating voltage of 15 kV to observe the coating morphology and to measure the coating thickness. A glancing incidence X-ray diffractometer (XRD, Rigaku- TTTRAX III) was employed to identify the coating structure with a Cu-target K α radiation at 40 kV and 30 mA and a glancing incident angle of 2°; the scanning angular (2θ) ranged from 20° to 80° at 2°/min. The chemical composition of the films was determined by the quantitative electron probe microanalysis (EPMA, JEOL JXA-8200) with the mode of line scanning for Ti, N, and O elements. A surface roughness analyzer (Mitutoyo SV-400) was applied to measure the average surface roughness (Ra value) for each specimen. Adhesion strength quality (ASQ) of the coatings was evaluated by using Rockwell-C indentation testing with a load of 1471 N [17]. The damage to the coatings was compared

with a defined ASQ basis, where the grades of HF1-HF4 were acceptable adhesion and HF5-HF6 represented insufficient adhesion (HF is the German short form for adhesion strength).

In addition, corrosive experiments were conducted in the air and divided two types: polarization test and immersion test. Moreover, the two corrosive media of 3.5 wt.% NaCl and 10 vol.% HCl solutions were selected for simulating the aggressive aqueous environment containing Cl⁻ ions. In the case of polarization tests, a potentiostat/galvanostat apparatus (EG&G model 263A, USA) was used to conduct corrosion tests and the 3.5 wt.% NaCl solution was selected as medium to simulate the sea water environment. A standard saturated calomel electrode (SCE) was used as a reference and platinum as a counter- or auxiliary electrode. The contact area in all cases was 1 cm², and the tests were carried out at ambient temperature. The electrode potential was raised from -0.5 V to 0.3 V at a scanning rate of 1 mV/s. All polarization curves were obtained after 30 min of free immersion of the specimens in order to stabilize the open circuit potential (OCP). Corrosion potential (E_{corr}) and corrosion current density (i_{corr}) values were further obtained by the polarization curve and the Tafel extrapolation method, respectively [18-20]. The percentage inhibition efficiency ($\psi_{pol}\%$) was calculated using the i_{corr} values to express the relation $\psi_{pol}\% = [(i_{corr} - i'_{corr}) / i_{corr}] \times 100$, where both i_{corr} and i'_{corr} are uninhibited and inhibited corrosion current densities, respectively [19, 20]. All the polarization tests were carefully

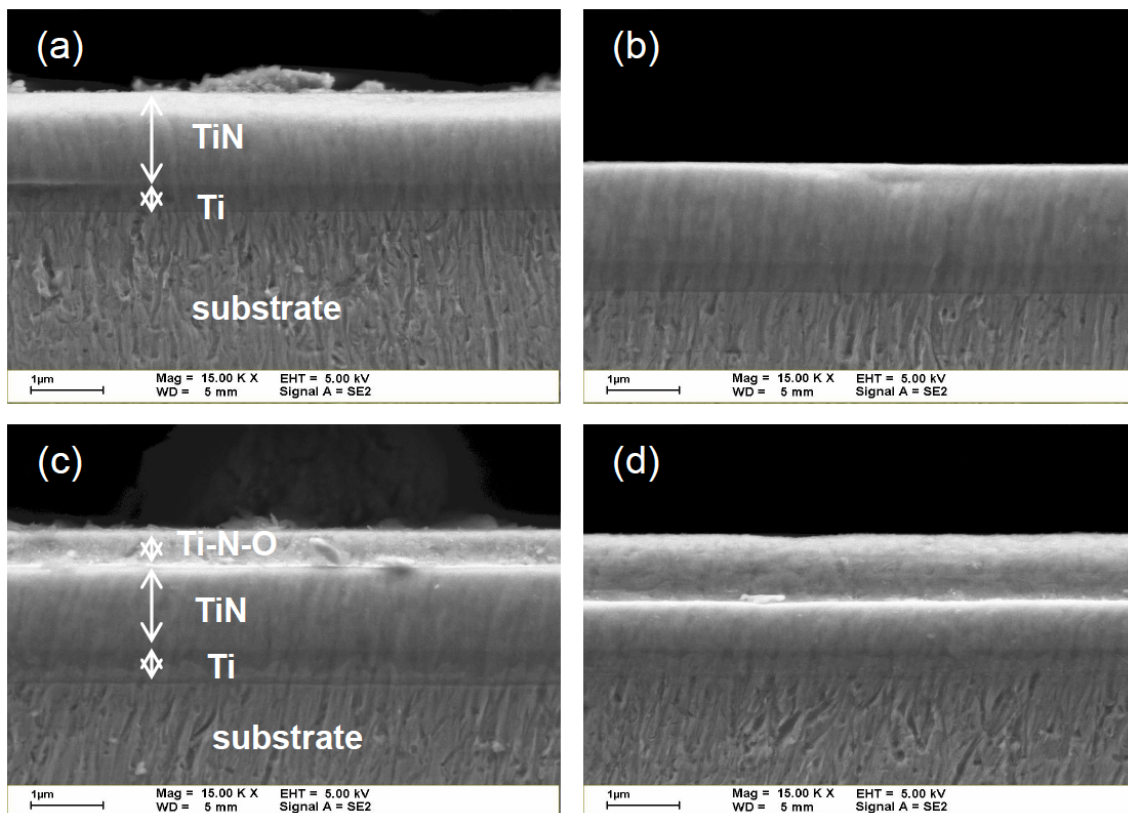


Figure 1: SEM Cross-sectional view of the coated specimens: (a) TiN, (b) TiN(400), (c) TiN(500), and (d) TiN(600).

carried out to avoid any scratch in the coatings. In the case of immersion tests, all the specimens were cleaned by using ultrasonic cleaning with alcohol before respectively immersed in 10 vol.% hydrochloric acid at room temperature. The weight loss was measured by using a micro-balance ($\pm 1 \times 10^{-4}$ g) at various time intervals. Also, the corroded surface of each specimen after corrosion tests was observed using SEM.

3. RESULTS AND DISCUSSION

3.1. Coating Structure and Composition

The study used FESEM to observe cross-sectional view of the TiN-coated specimens before and after post-heating treatment, as shown in Figure 1. From Figure 1a, it is observed that the coating had a columnar morphology, consisting of about 1.4 μm TiN film and 0.4 μm Ti-interlayer. After post-heating of 400 $^{\circ}\text{C}$ for 2 h, the TiN film almost had no variation in morphology (Figure 1b). It implied that the TiN film presented the well oxidation resistance at 400 $^{\circ}\text{C}$. When the post-heating temperature was up to 500-600 $^{\circ}\text{C}$, it was noted that a dense thin film of about 0.5-0.9 μm formed on the outward of the TiN-coated specimens. Moreover, the outer-layer in thickness had an increase while the thickness of original TiN film lessened with raising post-heating temperature, as shown in Figures 1c and d. Figure 2 compares the crystal structures of the coatings with and without post-heating in terms of the XRD patterns. The result showed that the un-annealed film had the main peaks on (111), (200), (220), and (311) diffracting planes for the TiN film because the depositing reaction between nitrogen and titanium ions formed a NaCl-type structure [21]. The XRD pattern of TiN(400) was almost the same with the un-annealed one. For the TiN(500) and TiN(600) films, there were some peaks of rutile-TiO₂ crystalline plane occurring in the XRD pattern besides the TiN peaks. Such the result

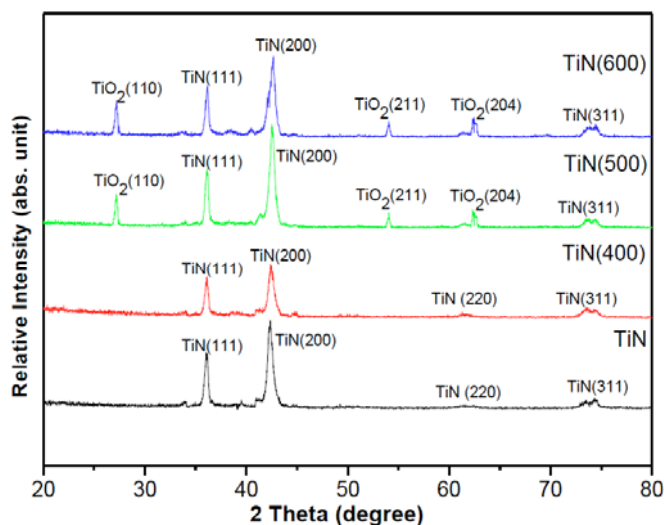


Figure 2: XRD patterns of the TiN coated specimens before and after annealing.

inferred that the outer-layer formed on the TiN(500) and TiN(600) specimens should be a Ti-N-O film, consisting of the rutile-TiO₂ and TiN phases. Moreover, the TiO₂ peaks in TiN(600) seemed to be stronger than that in TiN(500) due to the former with a thicker out-layer as compared to the latter (0.9 vs. 0.5 μm).

Chemical compositions of un-annealed and annealed coatings analyzed by EPMA are compared in Figure 3. For un-heated and heated at 400 $^{\circ}\text{C}$ conditions, both the coated specimens almost had the same contents for Ti (51.4 vs. 51.6 at.%) and N (48.6 vs. 48.4 at.%) elements in its Ti-N binary film. The result indicated that TiN film had the stable oxidation resistance under the post-heating temperature of 400 $^{\circ}\text{C}$. When the coated specimen was heated at 500 $^{\circ}\text{C}$, the oxygen content in the film was slightly higher than that of nitrogen (33.1 vs. 29.7 at.%). To further raise the post-heating temperature up to 600 $^{\circ}\text{C}$, the oxygen content in the film greatly increased (53.6 at.%) while both the nitrogen content (12.2 at.%) and the titanium content (34.2 at.%) decreased substantially. The result denoted that some of the nitrogen atoms were substituted by oxygen atoms to form TiO₂ in Ti-N-O outer-layer. That is, the affinity of titanium and oxygen is stronger than that of titanium and nitrogen [15]. We found, thickness and composition of the outer-layer depended on post-heating temperature. It is noticed that the Ti-N-O outer-layer in TiN(500) was thinner but more uniform than that in TiN(600) due to with the close content in Ti, N, and O elements.

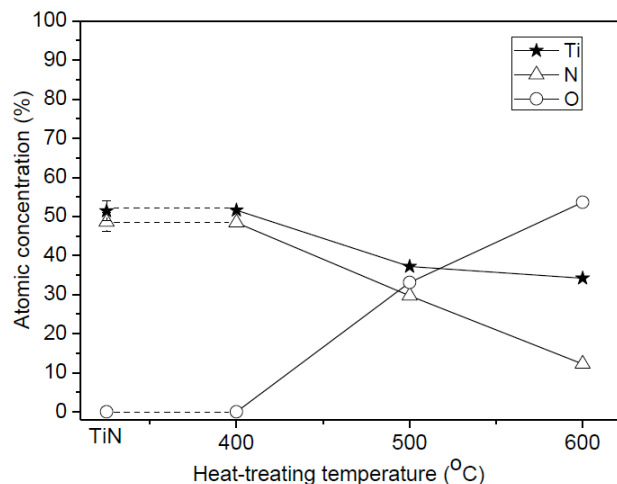


Figure 3: Effect of annealing temperature on the averaged concentration of the Ti, N, and O elements in the coating.

3.2. Analysis of Coating Roughness and Adhesion

In terms of surface roughness, the TiN coated specimen had a rougher surface than the uncoated one (R_a : 0.22 vs. 0.05 μm). The main reason for this phenomenon could be attributed to macro-particles deposited on the substrate by CAD process [22]. After post-heating, the surface roughness of TiN film had a slight decrease at 500 $^{\circ}\text{C}$ (R_a : 0.20 μm) but increased at 600 $^{\circ}\text{C}$ (R_a : 0.33 μm). The result should be

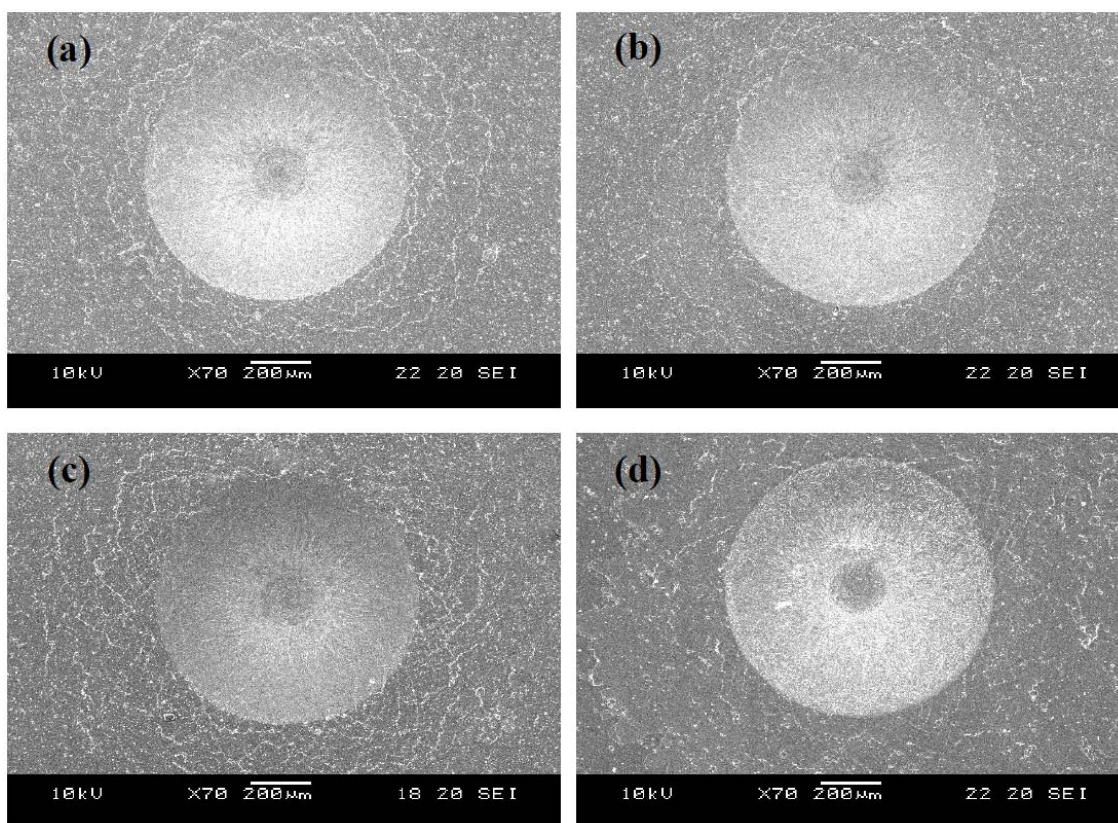


Figure 4: Fracture morphology of the coated specimens by Rockwell-C hardness tester: (a) TiN, (b) TiN(400), (c) TiN(500), and (d) TiN(600).

dependent upon atomic distribution in the Ti-N-O outer-layer. That is, the film with the more uniform composition tends to the lower Ra value. Indentation tests were performed by using the Rockwell-C hardness tests to evaluate the coating adhesion between film and substrate. According to the definition of ASQ as aforementioned [17], we found that all the TiN coated specimens had a clear and smooth indentation regardless of post-heating treatment, closely resembled HF1-HF2 grade (Figure 4). Accordingly, the post-heating for TiN film in this study seems to have no influence on the coating adhesion.

3.3. Analysis of Corrosion Behavior

Polarization tests for the uncoated 316L stainless steel, unheated TiN film, and the three heated films (TiN(400), TiN(500), and TiN(600)) were separately performed in 3.5

wt.% NaCl solution as aforementioned. Figure 5 shows the polarization curves (I_{corr} vs. E_{corr}) of these specimens after polarization tests, and all the data of polarization measurement obtained are listed in Table 1. Comparing to the uncoated substrate, the TiN coated specimens exhibited an increase in E_{corr} (-0.242 vs. -0.196 V_{SCE}). Further, it was found that the TiN film after post-heating could increase the E_{corr} value. Such the result implied that a steadier electrode potential was achieved and indicated an improvement on the corrosion resistance of 316L stainless steel via the coating and post-heating treatments. Particularly, TiN(500) had the highest E_{corr} value (-0.121 V_{SCE}) among the coated specimens. Corrosion current density (I_{corr}) was also calculated by using the Tafel equation [18], with a lower value reflecting better corrosion resistance. The result showed that the coated specimens had an evident improvement in corrosion resistance as compared to the uncoated one

Table 1: Data of Polarization Measurement for all the Specimens in this Study

Specimen	Electrode Potential, E_{corr} (V _{SCE})	Corrosion Current Density, I_{corr} ($\times 10^{-9}$ A/cm ²)	Inhibition Efficiency Ψ_{pol} (%)
Uncoated 316L	-0.242 ± 0.012	22.4 ± 1.1	---
Un-heated TiN	-0.196 ± 0.009	19.5 ± 0.1	12.9
TiN(400)	-0.139 ± 0.007	10.1 ± 0.5	54.9
TiN(500)	-0.121 ± 0.006	6.8 ± 0.3	69.6
TiN(600)	-0.126 ± 0.006	7.2 ± 0.4	67.8

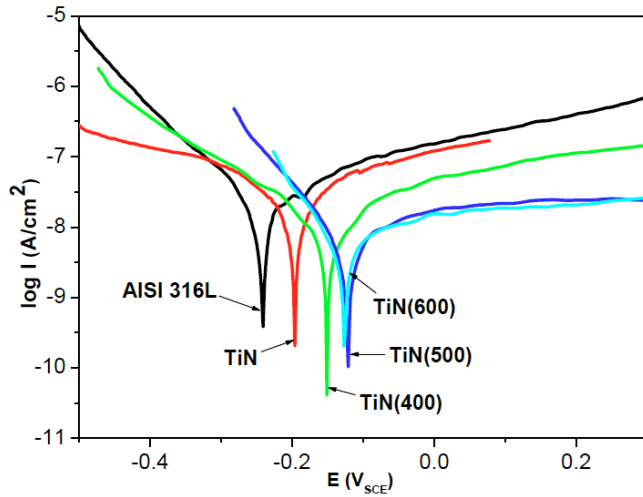


Figure 5: Polarization curves of the coated and uncoated specimens in 3.5 wt.% NaCl solution.

(22.4×10^{-9} A/cm²), where the i_{corr} values obtained for TiN, TiN(400), TiN(500), and TiN(600) were 19.5×10^{-9} A/cm²,

10.1×10^{-9} A/cm², 6.8×10^{-9} A/cm², and 7.2×10^{-9} A/cm², respectively. It is noted that TiN(500) had the lowest value to indicate the best corrosion resistance. Further, the inhibition efficiencies of corrosion for these coated specimens are listed in Table 1. It can be found that TiN(500) had the highest value up to 69.6%, followed by TiN(600), TiN(400), and finally TiN. Consequently, the corrosion resistance of them is in the order as follows: TiN(500)>TiN(600)>TiN(400)>TiN>316L. Figure 6 shows SEM micrographs of the specimens after the polarization test in 3.5wt.% NaCl solution. For the uncoated 316L stainless steel (Figure 6a), we can see a typical morphology of localized corrosion occurred on the surface but without pitting phenomenon. In the case of coated specimens with and without post-heating, the localized corrosion almost disappeared (Figures 6b-e). The result could verify that all the coated specimens had an improvement on corrosion protection as compared to the uncoated one.

Figure 7 shows weight loss of the uncoated and coated specimens with and without post-heating immersed in 10

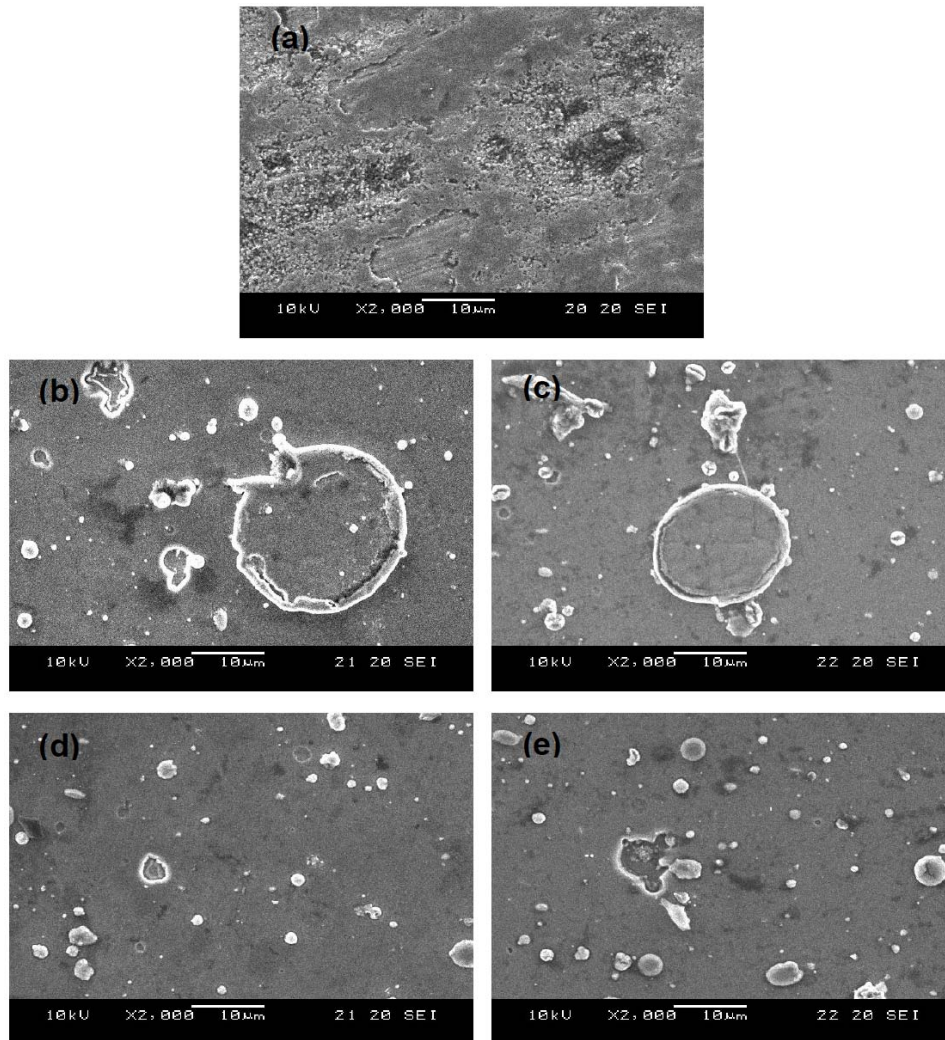


Figure 6: Surface morphology of the coated and uncoated specimens after polarization tests in 3.5 wt.% NaCl solution: (a) uncoated, (b) TiN, (c) TiN(400), (d) TiN (500), and (e) TiN(600).

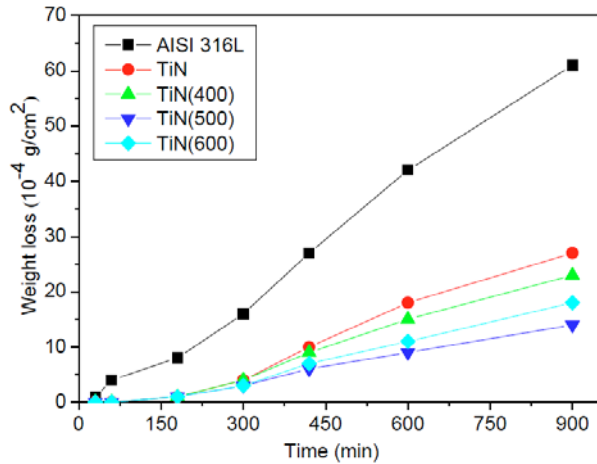


Figure 7: Comparison of weight loss of the various specimens in 10 vol.% HCl solution.

vol.% HCl solution at room temperature. We can see that the uncoated 316L stainless steel had a sharp weight loss because the reactions, $Fe \rightarrow Fe^{+2} + 2e^{-}$ and $2H^{+} + 2e^{-} \rightarrow H_2$,

took place rapidly in acid medium. In contrast, the coated specimens regardless of post-heating had well protective performance in corrosion resistance. In particular, the TiN(500) specimen efficiently mitigated the weight loss. Figure 8 further shows their SEM micrographs to prove the effect of the coatings on pitting corrosion of 316L stainless steel. It can be observed that the uncoated specimen after 900 min immersion tests in 10 vol.% HCl solution showed serious pitting corrosion (Figure 8a). After TiN coating and post-heating, the pitting phenomenon was eased up (Figures 8b-e). Particularly, the TiN (500) specimen nearly had no pitting. The reason could be attributed to homogeneous coatings consisting of TiN and Ti-N-O phases. Therefore, the optimal heated coating could effectively improve the pitting corrosion of 316L stainless steel in the study.

4. CONCLUSIONS

The TiN film arc-deposited on 316L stainless steel after post-heating at proper temperature could form a Ti-N-O outer-

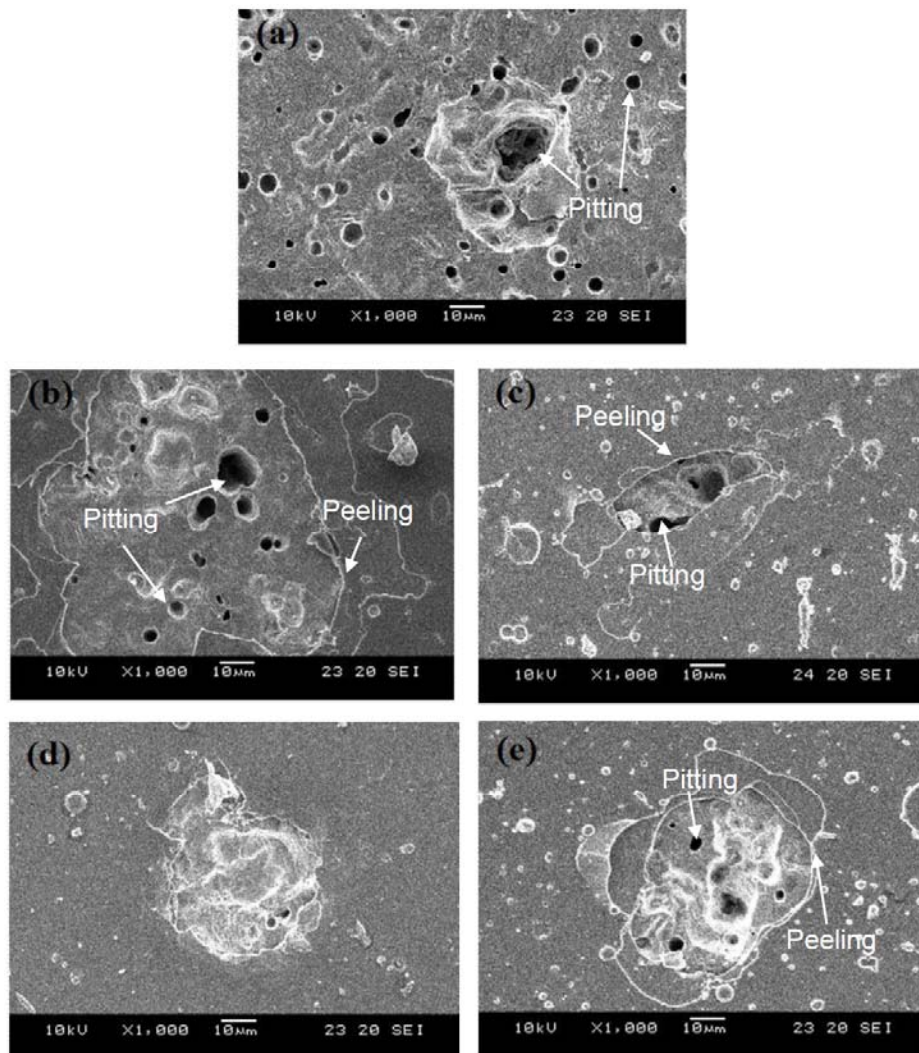


Figure 8: Surface morphology of the coated and uncoated specimens after 900 min immersion tests in 10 vol.% HCl solution: (a) uncoated, (b) TiN, (c) TiN(400), (d) TiN (500), and (e) TiN(600).

layer, consisting of rutile-TiO₂ and TiN phases. The outer-layer in thickness had an increase with raising the post-heating temperature. Moreover, the properties of the outer-layer such as composition, roughness, and adhesion were also dependent upon the heating temperature. When the heating temperature was controlled at 500 °C, the formed outer-layer had the most uniform composition among all the heated coatings. Such a post-heated film could remarkably reinforce the pitting corrosion resistance of 316L stainless steel.

ACKNOWLEDGEMENTS

The authors would like to thank the financial support of the National Science Council (Taiwan, ROC) under contract no. MOST 104-2221-E-036-001.

REFERENCES

- [1] Smith WF. Structure and Properties of Engineering Alloys, McGraw-Hill Inc., New York, 1993, p.288.
- [2] Lula RA. Stainless steel, ASM Ohio, 1986; p.150.
- [3] Peckner D. Bernstein IM, Handbook of Stainless Steel, McGraw-Hill Inc., New York, 1977; p.15-1.
- [4] Davison RM, DeBold T, Johnson MJ. Corrosion of Stainless Steels, Metals Handbook of ASM, 9th ed., 1980; Vol.13: p. 547.
- [5] John Sedriks A. Corrosion of Stainless Steel, John Wiley & Sons, Inc., New York, 1996; p.102.
- [6] Budinski KG. Surface Engineering for Wear Resistance, Prentice-Hall Inc., New Jersey, 1988; p.138.
- [7] Kok YN, Akid R, Hovsepian PEh. Tribocorrosion testing of stainless steel (SS) and PVD coated SS using a modified scanning reference electrode technique. *Wear* 2005; 259: 1472-81. <http://dx.doi.org/10.1016/j.wear.2005.02.049>
- [8] Dearnley PA, Mallia B. The chemical wear (corrosion-wear) of novel Cr based hard coated 316L austenitic stainless steels in aqueous saline solution. *Wear* 2013; 306: 263-75. <http://dx.doi.org/10.1016/j.wear.2012.09.002>
- [9] Nose M, Zhou M, Honbo E, Yokota M, Saji S. Colorimetric properties of ZrN and TiN coatings prepared by DC reactive sputtering. *Surface Coatings Technol* 2001; 142-144: 211-7. [http://dx.doi.org/10.1016/S0257-8972\(01\)01196-3](http://dx.doi.org/10.1016/S0257-8972(01)01196-3)
- [10] Endrino JL, Fox-Rabinovich GS, Gey C. Hard AlTiN, AlCrN PVD coatings for machining of austenitic stainless steel. *Surface Coatings Technol* 2006; 200: 6840-5. <http://dx.doi.org/10.1016/j.surfcoat.2005.10.030>
- [11] Leoni M, Scardi P, Rossi S, Fedrizzi L, Massiani Y. (Ti,Cr)N and Ti/TiN PVD coatings on 304 stainless steel substrates: Texture and residual stress. *Thin Solid Films* 1999; 345: 263-9. [http://dx.doi.org/10.1016/S0040-6090\(98\)01741-6](http://dx.doi.org/10.1016/S0040-6090(98)01741-6)
- [12] Wallén P, Hogmark S. Influence of TiN coating on wear of high speed steel at elevated temperature. *Wear* 1989; 130: 123-35. [http://dx.doi.org/10.1016/0043-1648\(89\)90227-5](http://dx.doi.org/10.1016/0043-1648(89)90227-5)
- [13] Chappé JM, Martin N, Lintymer J, Sthal F, Terwagne G, Takadom J. Titanium oxynitride thin films sputter deposited by the reactive gas pulsing process. *Appl Surface Sci* 2007; 253: 5312-6. <http://dx.doi.org/10.1016/j.apsusc.2006.12.004>
- [14] Vaz F, Cerqueira P, Rebouta L, *et al.* Preparation of magnetron sputtered TiN_xO_y thin films. *Surface Coatings Technol* 2003; 174-175: 197-203. [http://dx.doi.org/10.1016/S0257-8972\(03\)00416-X](http://dx.doi.org/10.1016/S0257-8972(03)00416-X)
- [15] Hsu CH, Huang KH, Lin YH. Microstructure and wear performance of arc-deposited Ti-N-O coatings on AISI 304 stainless steel. *Wear* 2013; 306: 97-102. <http://dx.doi.org/10.1016/j.wear.2013.07.005>
- [16] Hsu CH, Huang KH, Lin MR. Annealing effect on tribological property of arc-deposited TiN film on 316L austenitic stainless steel. *Surface Coatings Technol* 2014; 259: 167-71. <http://dx.doi.org/10.1016/j.surfcoat.2014.02.001>
- [17] Heinke W, Leyland A, Matthews A, Berg G, Friedrich C, Broszeit E. *Thin Solid Films* 1995; 270: 431. [http://dx.doi.org/10.1016/0040-6090\(95\)06934-8](http://dx.doi.org/10.1016/0040-6090(95)06934-8)
- [18] Uhlig HH. *Corrosion and Corrosion Control*, John Wiley & Sons Inc., New York, 1971; p. 45.
- [19] Jacob KS, Parameswaran G. Corrosion inhibition of mild steel in hydrochloric acid solution by Schiff base furoin thiosemicarbazone. *Corrosion Sci* 2010; 52: 224-8. <http://dx.doi.org/10.1016/j.corsci.2009.09.007>
- [20] Hsu CH, Chen ML. Corrosion behavior of nickel alloyed and austempered ductile irons in 3.5% sodium chloride. *Corrosion Sci* 2010; 52: 2945-9. <http://dx.doi.org/10.1016/j.corsci.2010.05.006>
- [21] Pierson HO. *Handbook of Refractory and Nitrides*, Noyes Publications, New Jersey 1996; p.156. <http://dx.doi.org/10.1016/B978-081551392-6.50010-6>
- [22] Hsu CH, Lee CC, Ho WY. Filter effects on the wear and corrosion behaviors of arc deposited (Ti,Al)N coatings for application on cold-work tool steel. *Thin Solid Films* 2008; 516: 4826-32. <http://dx.doi.org/10.1016/j.tsf.2007.09.017>